Int. J. Solids Structures Vol. 20, No. 11/12, pp. 921–934, 1984
Printed in the U.S.A.

0020-7683/84 $3.00 + .00
Pergamon Press Ltd.

A ONE-DIMENSIONAL VISCOPLASTIC CONSTITUTIVE THEORY FOR FILLED POLYMERS

RICHARD V. BROWNING
Los Alamos National Laboratory, Los Alamos, NM 87544, U.S.A.

and

MORTON E. GURTIN and WILLIAM O. WILLIAMS
Department of Mathematics, Carnegie-Mellon University, Pittsburgh, PA 15213, U.S.A.

(*Received* 6 *December* 1982; *in revised form* 26 *September* 1983)

INTRODUCTION

Certain highly filled polymeric materials, such as those used in solid propellants and high explosives, exhibit uniaxial behavior of the type illustrated by Fig. 1.† Although a linear viscoelastic material would produce this form of stress–strain curve, a relaxation function which reproduces the loading curve predicts much smaller values of the offset strains ϵ_1, ϵ_2 than those observed. In addition, it is frequently found that the offsets include a permanent part, a feature not characteristic of linear viscoelastic solids, for which the equilibrium modulus is nonzero. Alternatively, an elastic-plastic material with very small yield stress and extreme work-hardening would exhibit a similar stress–strain picture, without the hysteresis, but would not show the creep and relaxation typical of these materials.

The first attempt to model such filled polymers was by Farris and Fitzgerald[1], who utilized L^p-norms of the strain history to characterize internal damage, which is thought to be the cause of the plastic behavior described above. Later, Quinlan[8] introduced a theory in which this damage is described by an internal state variable whose evolution is governed by an ordinary differential equation, while Swanson, Christensen, and Christensen[9] proposed a model in which the stress is a viscoelastic term multiplied by an affine function of ϵ/ϵ_m, where ϵ is the strain and ϵ_m its past maximum.‡

The chief problem with the models developed by Farris, Fitzgerald, and Quinlan is their complex nature, a factor which renders intuitive insight difficult and which leads to a complicated program for the characterization of real materials. Indeed, all previous characterizations using these models [2, 3, 11] have been based on least-squares procedures applied to a large experimental base, with the entire base being used to determine the underlying constants. As is well known, procedures of this type can lead to large errors when the model is extrapolated outside of the experimental range.

Our purpose here is to develop a simple constitutive model for the materials discussed above. We base this model on the following two hypotheses:

(i) There is a constitutive quantity, called the pseudo-stress π, which is related to the strain through an elastic–plastic stress–strain law.

†See [1–6]. There is a large literature on *viscoplastic* materials, which display similar characteristics of yield and flow; the underlying constitutive equations, however, are completely different from those presented here. (See [7].)

‡Earlier, Mullins[10] discussed a rate-independent constitutive equation giving the strain when the stress and its past maximum are known, while Farris[2] and Gurtin and Francis[6] introduced similar models based on the past maximum of strain. A different approach is taken by Schapery[12], who models damage in terms of the growth and healing of flaws.

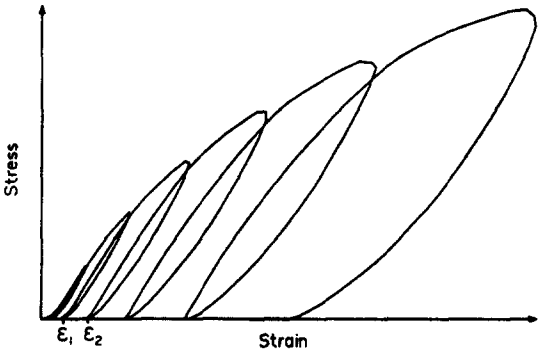

Fig. 1. A typical experimental stress-strain diagram (here for PBX-9502).

(ii) The true stress σ is related to π through a linear viscoelastic law.

In this way the entire rate-dependent portion of the response is characterized by the relaxation function of (ii) superposed over a rate-independent plastic behavior.†

We describe a systematic process for determining the relaxation function and the two functions characterizing the plastic response from a series of three types of tests. We illustrate our methods by application to three different materials: two plastic-bonded explosives and an inert structural replica of such explosives.

1. THE MODEL

Keeping in mind the stress–strain‡ behavior illustrated in Fig. 1, we first introduce a constitutive equation describing one-dimensional compressive§ loading of an elastic–plastic material. Thus we write

$$\pi = F(\epsilon, \epsilon_m), \tag{1}$$

where $\pi = \pi(t)$ is the compressive *stress* at time t, $\epsilon = \epsilon(t)$ is the compressive *strain* at t and¶

$$\epsilon_m(t) = \max_{0 \le s \le t} \epsilon(s) \tag{2}$$

is the *past maximum of strain*.

Since we ascribe the plastic behavior to internal damage of the material, we shall apply the adjective *virgin* to states in which $\epsilon = \epsilon_m$ and *damaged* to those with $\epsilon < \epsilon_m$. Thus we refer to the loading curve

$$\pi = g(\epsilon) = F(\epsilon, \epsilon) \tag{3}$$

as the *virgin curve*. We then rewrite (1) as

$$\pi = g(\epsilon_m) f(\epsilon, \epsilon_m) \tag{4}$$

and call f the *damage function*. Note that

$$f(\epsilon_m, \epsilon_m) = 1 \tag{5}$$

†Gurtin, in [13], originated the idea of superposition of linear viscoelasticity to isolate rate effects; the particular formulation of [13], based on the inverse (strain-stress) relation, does not lend itself to modeling permanent deformation.

‡Here stress is (force)/(original area), while the strain is (change in length)/(original length).

§For convenience we do not discuss tensile loading, which could be similarly modeled. The materials we discuss are typically quite weak in tension and hence the compressive regime displays the most markedly inelastic behavior.

¶Here and in what follows we assume that $\epsilon(t) = 0$ for $t < 0$.

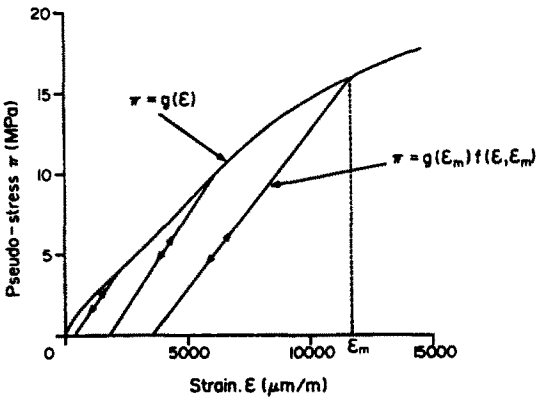

Fig. 2. The envelope represents the virgin curve, while the lower segments represent unloading and reloading while damaged. The material is 900–10.

and that we presume loading and unloading in the damaged regime to occur on the same path. These constitutive relations are illustrated in Figure 2, which is taken from a test on the real material 900–10 discussed later.

To introduce rate dependence into the model we shall regard π as a *pseudo-stress*† and relate it to the *stress* σ by a linear viscoelastic law:

$$\sigma(t) = \int_0^t G(t-s)\dot{\pi}(s)\,ds, \tag{6}$$

with G the *stress-relaxation function*. Of course we may eliminate π from (6) to obtain

$$\sigma(t) = \int_0^t G(t-s)\frac{d}{ds}F(\epsilon(s), \epsilon_m(s))\,ds. \tag{7}$$

We note that G is accessible to a standard stress-relaxation test: if $\epsilon(t) = \epsilon_0$ for all $t > 0$, then the corresponding stress $\sigma_{\epsilon_0}(t)$ is given by

$$\sigma_{\epsilon_0}(t) = g(\epsilon_0)G(t). \tag{8}$$

If we normalize g so that $g(\epsilon_0) = \epsilon_0$, then we obtain G as $\sigma_{\epsilon_0}(t)/\epsilon_0$.

2. CREEP FORMULATION

Although the model is most easily visualized as presented in Section 1, frequently it is useful to have it reformulated using a functional which gives the strain in terms of the stress history. Indeed, our experimental characterization is based on such a formulation.

Suppose that G is smooth (with $G(0) > 0$). Then we may solve

$$G(0)J(t) + \int_0^t \dot{G}(s)J(t-s)\,ds = 1 \tag{9}$$

to obtain the (unique) *creep function* J, and using J equation (6) may be inverted to give

$$\pi(t) = \int_0^t J(t-s)\dot{\sigma}(s)\,ds. \tag{10}$$

Correspondingly, if we suppose that

$g(\epsilon)$ is continuous and strictly increasing,
$f(\epsilon, \epsilon_m)$ is strictly increasing in ϵ for fixed ϵ_m,

†In practice it is convenient to render π dimensionless so that the relaxation function has the customary units. Thus it would not be inappropriate to regard π as a pseudo-strain, as may be seen in what follows.

we may write

$$\epsilon = k(\pi_m)h(\pi, \pi_m), \tag{11}$$

where π_m is the past maximum of π. Again k, which is the inverse of g, describes the *virgin response* while h, which obeys

$$h(\pi_m, \pi_m) = 1, \tag{12}$$

is the *damage function*. (We will establish the existence of the inverse relation (11) at the end of this section.) We shall have occasion to use the *nonlinearity function* $\tilde{k}$ defined by

$$\tilde{k}(\pi) = \frac{k(\pi)}{\pi}. \tag{13}$$

Consider now a standard creep test. If $\sigma(t) = \sigma_0$ for all $t > 0$ then the corresponding pseudo-stress π_0 is

$$\pi_0(t) = \sigma_0 J(t) \tag{14}$$

and the strain $\epsilon_{\sigma_0}(t)$ is given by

$$\epsilon_{\sigma_0}(t) = k(\sigma_0 J(t)). \tag{15}$$

Thus

$$\frac{\epsilon_{\sigma_0}(t)}{\sigma_0} = \tilde{k}(\sigma_0 J(t))J(t) \tag{16}$$

and as σ_0 goes to zero,

$$\lim_{\sigma_0 \to 0} \frac{\epsilon_{\sigma_0}(t)}{\sigma_0} = \tilde{k}(0)J(t). \tag{17}$$

Thus at small values of stress the usual computation of linear viscoelasticity theory may be expected to return an approximation to $J(t)$, justifying our use of the term creep function.

Finally, let us establish the existence of k and h, and the validity of (11) as inverse to (4). We assume that $\epsilon(t)$, and hence also $\pi(t)$, is piecewise continuous. First note that

$$\pi_m(t) = \max_{s \le t} g(\epsilon_m(s)) f(\epsilon(s), \epsilon_m(s)) = \max_{s < t} g(\epsilon_m(s)), \tag{18}$$

since $f(\epsilon, \epsilon_m) \le 1$ and $f(\epsilon_m, \epsilon_m) = 1$. But since g and ϵ_m are continuous and non-decreasing,

$$\pi_m(t) = g(\max_{s \le t} \epsilon_m(s)) = g(\epsilon_m(t)), \tag{19}$$

and as g is strictly increasing we may invert this relation:

$$\epsilon_m(t) = k(\pi_m(t)). \tag{20}$$

Next, we redefine f to find

$$\hat{f}\left(\frac{\epsilon}{\epsilon_m}, \epsilon_m\right) = f(\epsilon, \epsilon_m). \tag{21}$$

Then

$$\pi(t) = g(\epsilon_m(t))f(\epsilon(t),\epsilon_m(t)) = \pi_m(t)\hat{f}\left(\frac{\epsilon(t)}{\epsilon_m(t)}, \epsilon_m(t)\right). \tag{22}$$

Thus

$$\frac{\pi(t)}{\pi_m(t)} = \hat{f}\left(\frac{\varepsilon(t)}{\varepsilon_m(t)}, \varepsilon_m(t)\right). \tag{23}$$

But $\hat{f}$ is strictly increasing in its first argument, so we may invert this to

$$\frac{\epsilon(t)}{\epsilon_m(t)} = \hat{h}\left(\frac{\pi(t)}{\pi_m(t)}, \epsilon_m(t)\right) \tag{24}$$

and set

$$h(\pi, \pi_m) = \hat{h}\left(\frac{\pi}{\pi_m}, k(\pi_m)\right) \tag{25}$$

to obtain the desired relation.

3. CHARACTERIZATION

Here we describe, in general terms, a procedure for characterizing the response of a material presumably modeled by this constitutive theory.

(*i*) *Determination of the relaxation function or creep function*

Consider first a relaxation test. Then (8) yields

$$\frac{\sigma_{\epsilon_0}(t)}{\epsilon_0} = \tilde{g}(\epsilon_0)G(t), \tag{26}$$

where $\tilde{g}(\varepsilon) = g(\varepsilon)/\varepsilon$ measures the deviation from linearity. Normalizing by $\tilde{g}(\varepsilon_0) = 1$ we obtain a value for G. A useful test of the accuracy of the model is to run several tests at different values of strain $\varepsilon_1, \varepsilon_2, \ldots$ and then to verify that

$$\frac{\sigma_{\epsilon_i}(t)/\epsilon_i}{\sigma_{\epsilon_j}(t)/\epsilon_j} \tag{27}$$

is independent of time.

The corresponding creep test is intrinsically less accurate; eqn (16) gives

$$\frac{\epsilon_{\sigma_0}(t)}{\sigma_0} = \tilde{k}(\sigma_0 J(t))J(t) \tag{28}$$

with a factor $\tilde{k}(\sigma_0 J(t))$ which is predicted to vary in time. If J is bounded and σ_0 sufficiently small, by (17), the error induced by taking $\epsilon_{\sigma 0}(t)/\sigma_0$ to be J may perhaps be negligible.

In any case it is possible to obtain either G or J from the other by solving (9). Of course this may be expected to introduce numerical errors.

The creep function J must be available to use in evaluating the remaining tests.

(*ii*) *Determination of the virgin response*

Experiments involving monotonic loading now suffice to determine the functions g and k. Taking the creep function J found in part (*i*), one may integrate it together with the

experimental $\sigma(t)$ to obtain $\pi(t)$. Then a plot of $\pi(t)$ versus the experimental $\epsilon(t)$ reveals the form of g. In principle a single experiment suffices, but a useful test of the constitutive hypothesis that J encompasses the entire rate dependence is afforded by taking a series of such tests at differing rates and comparing the corresponding graphs.

(iii) Determination of the damage function

To determine the damage function it is necessary to have experiments involving unloading, and, optimally, reloading, processes utilizing a large selection of values of ϵ_m or π_m. For example loadings such as those shown in Figs. 4 and 11 may be used. From the experimental $\sigma(t)$ one uses (10) to compute $\pi(t)$ and then considers a π–ϵ plot over each interval on which ϵ_m is constant and $\epsilon < \epsilon_m$. The corresponding π–ϵ plots, each for a different value of ϵ_m, may be used to construct $f(\epsilon, \epsilon_m)$ by a two-variable fitting process.

Finally, note that to increase the accuracy of the numerical integrations necessary to compute π one could utilize tests of the form shown in Fig. 4, with the period between the spikes sufficiently large to allow complete relaxation, so that the integration need be performed only over each isolated spike.

4. TEST MATERIALS AND METHODS

Test materials

Most of our results concern an inert plastic-bonded material known as 900–10, which is often used as a substitute for explosives in structural tests. It contains 46% barium nitrate, 48% pentaerythritol, 2.8% cellulose nitrate, 3.2% tris beta chloroethyl phosphate and 0.5% red dye by weight.

The second material studied is PBX-9502, a plastic bonded explosive. The material is 95% triaminotrinitrobenzine (TATB), an organic explosive in the form of fine crystals, bound together with 5% Kel-F800, a plastic, namely poly(trifluorochloroethylene).

The third material is PBX-9501, another plastic-bonded explosive. This material is 95% tetranitro-tetraazacyclooctane (HMX), an organic crystalline compound, 2.5% Estane 5740, a polyurethane binder, and 1.25% each of the plasticizers bis(2,2 - dinitropropyl) acetal/bis(2,2 - dinitropropyl) formal (BDNPA/BDNPF).

Test methods

Specimens were 41.3 mm dia. by 50.8 mm long cylinders usually instrumented with both bonded strain gages and clip-on extensometers. The relatively low length-to-diameter ratio suggests a possible problem with end-effects. However the bonded strain gages were located on the specimens at the mid-point, and we used an elastic finite-element analysis to deduce that the measured strains would not be seriously affected by the lateral frictional restraints on the ends of the specimen, except near failure. Failure loads and strains near failure condition could of course greatly be influenced by the end conditions. The strain gages were 1/4″ gage length biaxial gages mounted on opposite sides of the specimen. Extensometers with 25 mm gage length were mounted straddling the strain gages. The extensometers tend to exhibit hysteresis under reverse loading conditions, an effect that became apparent when comparing the extensometer and strain gage results. Because of the hysteresis and the enhanced end effects with the extensometers, we customarily used the strain gage results.

There are two exceptions to this duplicate instrumentation method. In most early tests only axial extensometers were used,† while creep data were obtained using only bonded strain gages due to space limitations in the creep apparatus.

The constant-rate-to-failure and cyclic-load tests were all performed on a screw-driven, servo-controlled, constant-rate testing machine. Early creep tests were done using a lever-arm compression tester, while later tests were done in dead-weight loading frames using a compression cage.

†These early tests were done by R. Peeters and the techniques used are described in [14].

Data acquisition methods

A data acquisition system driven by a desk top calculator was used to apply pulsed excitation to the various strain gages and then to read the bridge output signals. The voltage readings from the bridge were stored on a floppy diskette before being transferred to a general purpose computer for conversion to strain values and correction for thermal effects and finally for display and manipulation as described below.

Construction and testing of a model

A typical experimental stress-strain graph for 900–10 was already given in Fig. 1; the corresponding results for PBX-9501 and PBX-9502 are essentially the same. Our tests did not include stress-relaxation; hence we used the characterization in terms of J.

Simultaneous with this characterization we also constructed *linear viscoelastic* and *elastic–plastic* models, a simple procedure within our framework: a linear viscoelastic material has $\epsilon(t) = \pi(t)$, while for an elastic–plastic material J is a constant.

The data, available in digital form as the 'experimental' functions $\sigma(t)$, $\epsilon(t)$, $t \geq 0$ showed typical irregularities. Hence each function J, g, f measured from experimental data was smoothed using a least-squares fit in spline functions. Care was taken to ensure that the error induced by the approximation is insensible in comparison with the experimental and sample-to-sample errors. The latter errors were quite difficult to reduce. The materials are quite temperature sensitive, and many tests were run at a highly variable "room temperature". Corrections for thermal expansion were made, but of course the functions J, g, f may be expected to be temperature dependent. Further, the variation in properties from one batch of materials to the next was significant and difficult to control.

Evaluation errors may be expected to arise mainly from two sources. The first is due to the inaccuracy inherent in using creep data to approximate J, as previously discussed. The second source of error is the numerical integration necessary for the computation of π from σ. There is reason to be suspicious both of very short time computations, in which the experimental scatter in σ and ε due to start-up problems lead to integration errors, and of long time computations, in which any computationally-practical mesh spacing is rather coarse.

We now discuss, in detail, the characterization of 900–10.

The evaluation of J was from creep tests at stress levels of 1–3 MPa. A spline fit with knots spaced uniformly in each decade except the first and logarithmically there proved quite acceptable.

Ramp tests were performed at three crosshead speeds, each a decade apart and the test at the middle rate was used to determined the virgin curve k. The faster and slower tests were then used as consistency checks (Fig. 3); these results will be discussed at the end of this section.

The virgin curve $\epsilon = k(\pi)$ determined in this way exhibited erratic behavior near $\pi = 0$; to overcome this problem the value of the slope $k'(0)$ was chosen so as to give good agreement with the creep test used to determine J.

The damage function h was determined as discussed above using the test shown in Fig. 4. It was found that a damage function $h(\pi, \pi_m)$ linear in π gave a satisfactory fit to the data. There were two obvious model errors visible in our construction of h, each of which may be removed only at the cost of great complexity and hence was allowed to stand. First, the experimental damage curves showed hysteresis, an effect not predicted by our model.† Second, it was found in the experiments that $f(\epsilon_m, \epsilon_m)$ is not always equal to 1 (see (5)); in detail, π does not always return precisely to π_m as ε returns ε_m, but only attains the virgin curve after a small continued loading. (The discrepancy was less than 15% of the total strain value.)

Overall it was felt that no gross defects of the model appeared in the process of its evaluation. To test the model we considered other experiments and computed the strain by applying J, h, and k to the experimental stress history σ. The complete set of

†That is, a hysteresis in the *elastic–plastic* part of the response above and beyond the hysteresis predicted by the *viscoelastic* part of the response.

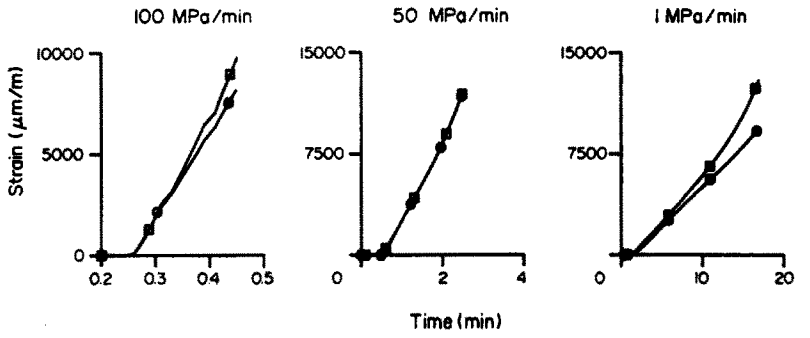

Fig. 3. Experimental (○) and calculated (□) responses of 900–10 to stress ramps at various rates of loading.

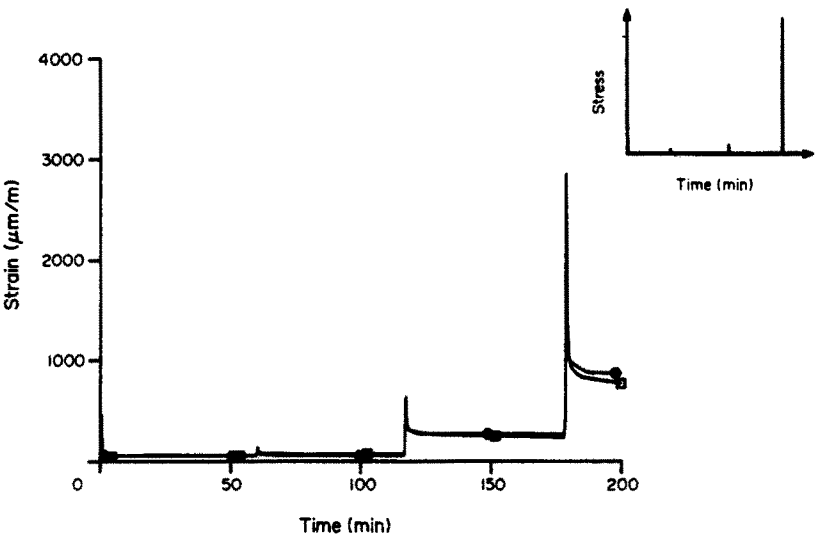

Fig. 4. Experimental (○) and calculated(□) response for 900–10. The stress rate is 10 MPa/min.

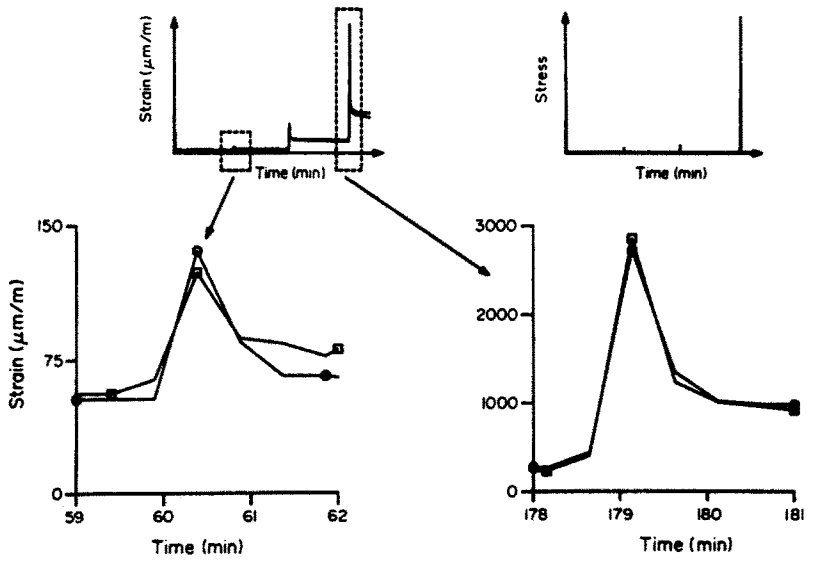

Fig. 5. Experimental (○) and calculated (□) response for 900–10. The stress rate is 10 MPa/min.

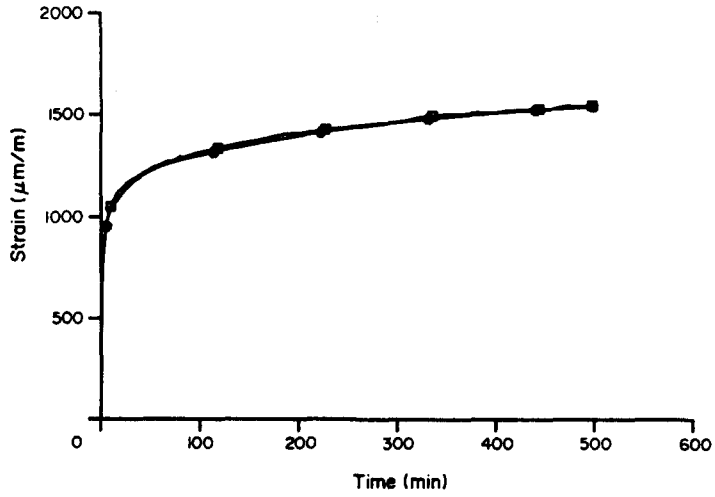

Fig. 6. Experimental (O) and computed (□) strains for a creep test on 900–10.

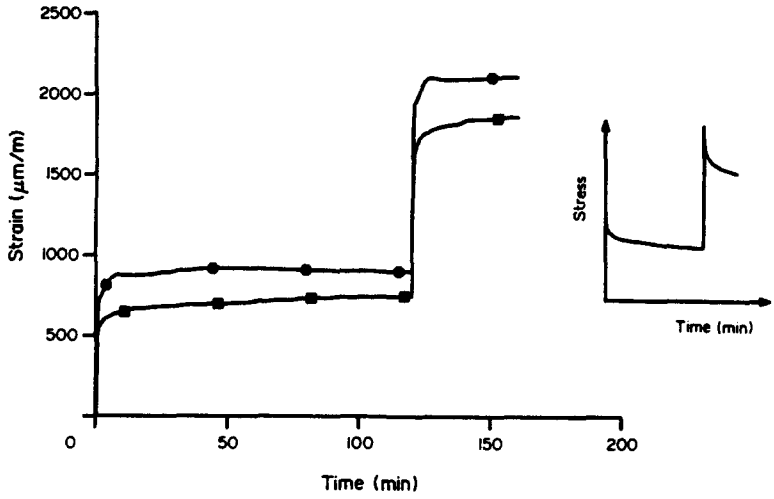

Fig. 7. Comparison of experimental (O) and calculated (□) response for 900–10. The stress-rate is 10 MPa/min.

comparisons consists of Figs. 3–7. As seen from Fig. 6, our model accurately predicts creep response.

The comparisons for the ramp tests show greater variability. The predictions for the test at 50 Mpa/min, which was used in the characterization process, are—as to be expected—excellent. The agreement for the fastest test is superior to that for the slowest, for which the predictions are not very good at the higher strain levels. These tests indicate rate effects in the virgin curve different from those embodied in the creep function. It should be born in mind, however, that these tests cover three decades, a nontrivial time-span. The discrepancy could also be caused by sample-to-sample variation.

The predictions for the repeat sawtooth test (Figs. 4 and 5) are excellent. This test was used to characterize the damage function and indicate that our method of modelling damage is reasonable, as is our assumption of linear damage-curves. The portions of this test not containing damaged states were not used in the characterization procedure, and the excellent agreement there is reassuring.

The comparison of theory and experiment for the two-stage stress-relaxation test (Fig. 7) is not as good as the previous comparisons. The cause of the large discrepancies is the first jump in strain, for which our predictions are far too high. However, this portion of the test corresponds to extremely low amplitudes, while our characterization procedure

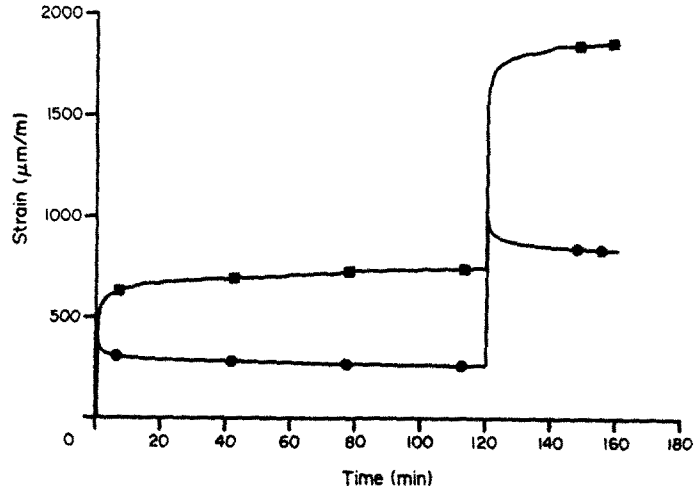

Fig. 8. Elastic-plastic model experimental (○) and calculated (□) response for the test shown in Fig. 7.

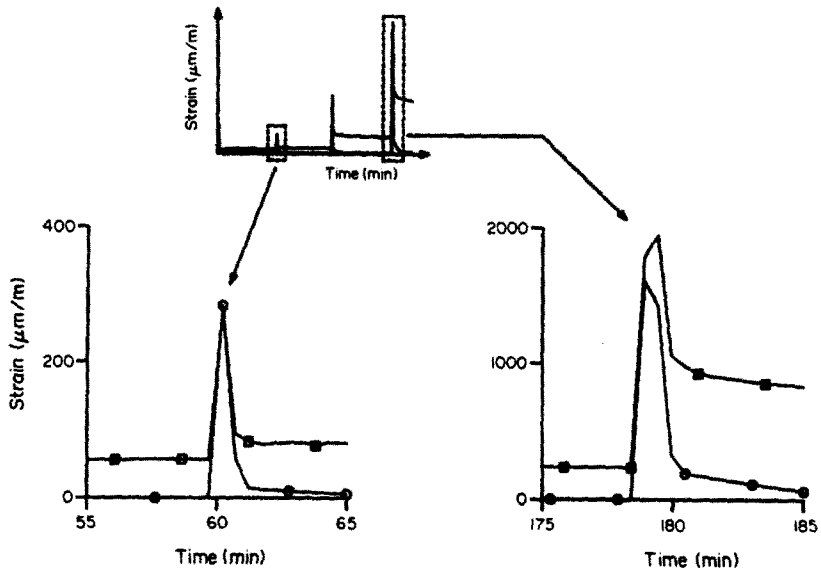

Fig. 9. Linear viscoelastic model experimental (○) and calculated (□) response for the test shown in Fig. 5

concentrated on large-amplitude behavior. Further, as mentioned previously, the ramp tests indicated somewhat erratic behavior at small strains, possibly due to initiation errors in the experiments. The response following the second jump is also in error, but this error is probably due to the discrepancy in the first jump. If the calculated amplitude is lowered by an amount equal to the discrepancy at the start of the second jump, then the resulting error at $t = 162$ min. is less than 5%.

Elastic–plastic and linear viscoelastic models were also determined for the material 900–10, and typical comparisons are shown in Figs. 8 and 9. These models did not characterize the material at all well: the elastic–plastic model led to erroneous results for long-term stress relaxation (see Fig. 8), while the linear viscoelastic model did not yield the requisite permanent offset (see Fig. 9).

Using the foregoing procedure we characterized the explosive PBX-9502. This material was only slightly viscoelastic, and the comparisons between theory and experiment were uniformly excellent—far better than that for 900–10. Figures 10 and 11 indicate such comparisons; these tests were not used to characterize the material. Similar results were

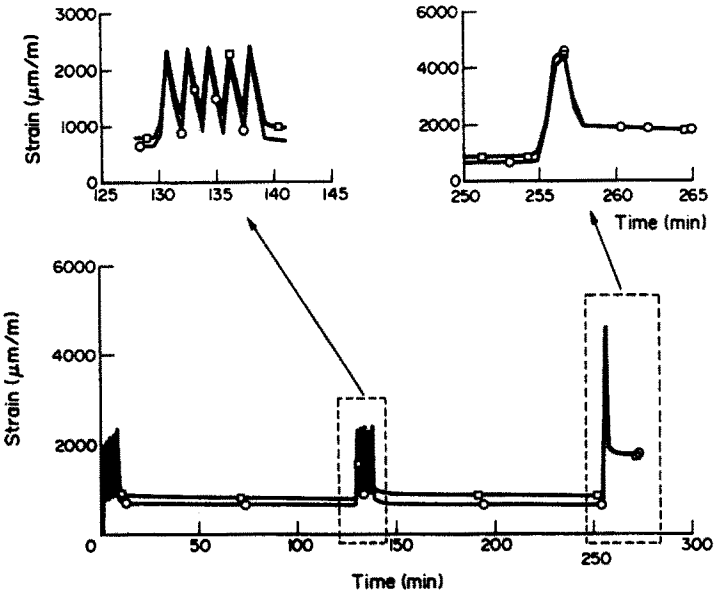

Fig. 10. Experimental (O) and calculated (□) strain for PBX-9502. The stress rate is 5 Mpa/min.

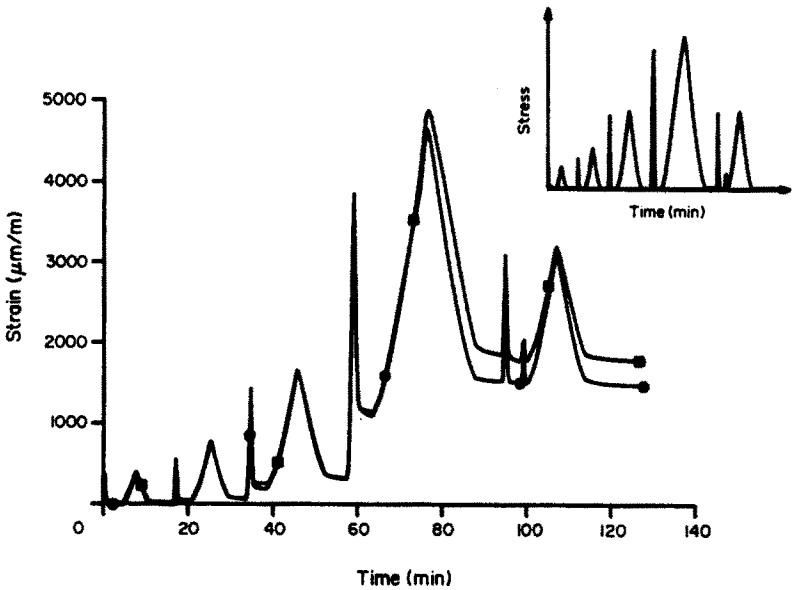

Fig. 11. Comparison of experimental (O) and calculated (□) strains for PBX-9502. The stress rates are 5 and 0.5 MPa/min.

obtained for the explosive PBX9501, which shows less permanent deformation but is much more viscoelastic than 9502; see Figs. 12–15. Again none of the tests plotted were used in the characterization.

Figure 16 illustrates the difference in the response of the three materials.

CONCLUSIONS

The three materials modeled are similarly constituted but display behavior ranging from relatively elastic (PBX-9502) to quite viscous (PBX–9501). Thus we feel that they provide a good test of the model and of the modeling procedure. Reviewing the results we feel that the model offers a quite good, through not excellent, fit to these materials. The chief advantage of this model is its relative simplicity. Characterization can be obtained from one creep test, one ramp loading test, and one multiple loading-unloading

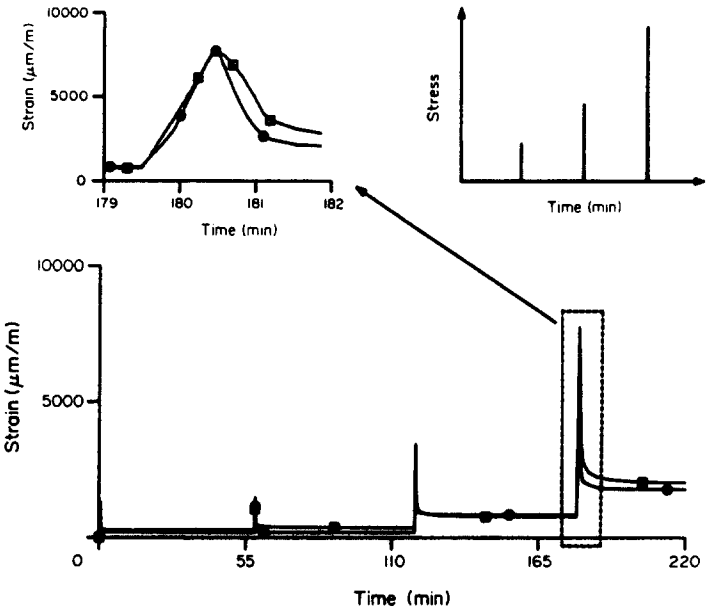

Fig. 12. Experimental (○) and calculated (□) response for PBX-9501. The stress rate is 5 MPa/min.

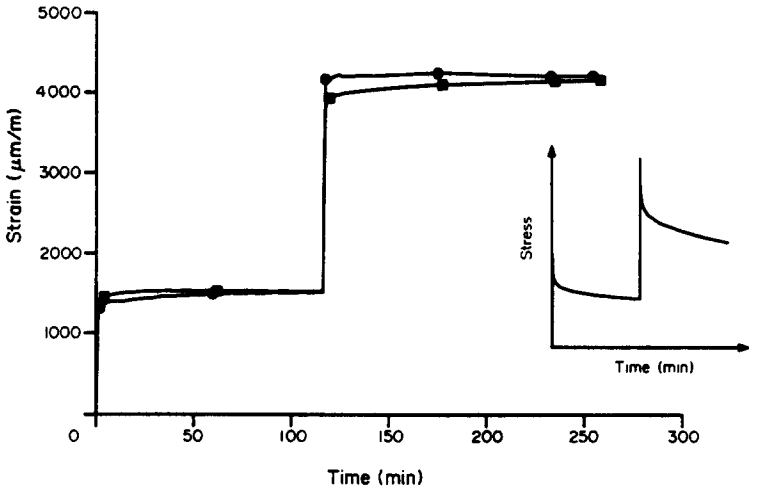

Fig. 13. Experimental (○) and calculated (□) response for PBX-9501. The stress rate is 5 MPa/min.

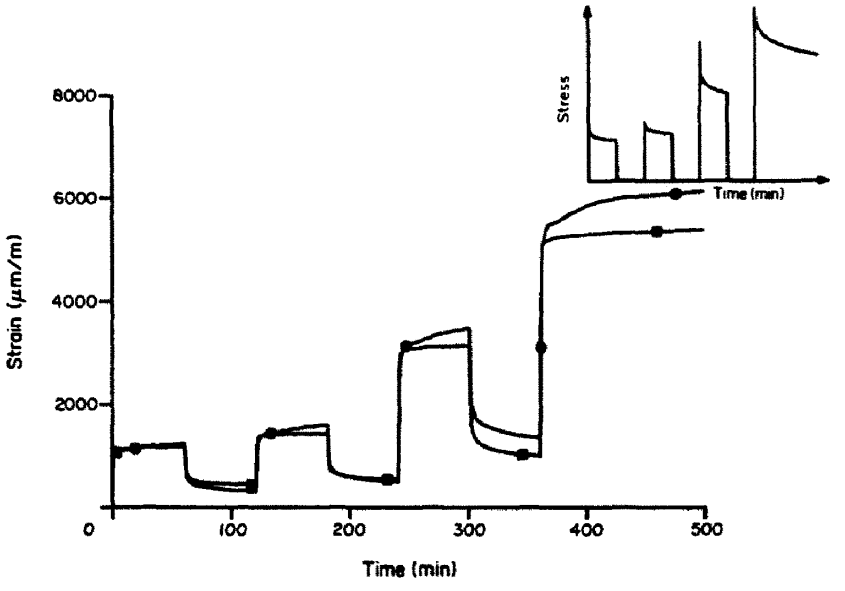

Fig. 14. Experimental (O) and calculated (□) response for PBX-9501.The stress rate is 5 MPa/min.

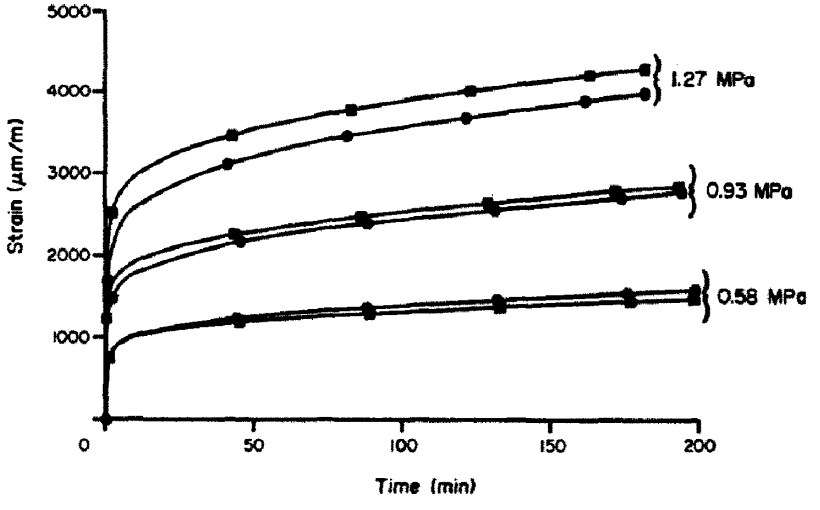

Fig. 15. Comparison of experimental (O) and calculated (□) response for creep tests at three levels. The material is PBX-9501.

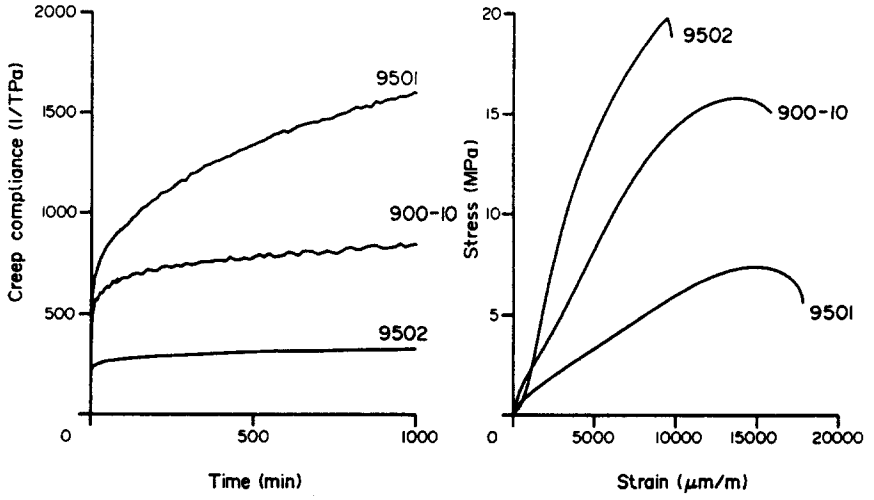

Fig. 16. Comparison of creep compliance and constant rate loading (at compatable strain rates) for the three materials modeled.

test, and these three, with perhaps six or eight more to test against, would constitute a complete one-dimensional test program. An extension to three-dimensional loading, which we are now testing, can be made relatively easily from one more series of tests.

The defects of the model seem to lie mostly in situations involving long term stress relaxation (Figs. 7 and 14). We feel that this is intrinsic to the model and could be eliminated only by introducing relations between σ and π much more elaborate than (6); it is not clear that in applications the increase in accuracy could justify the corresponding increase in complexity.

Acknowledgements—This work was supported by the Los Alamos National Laboratory, the National Science Foundation, and the Army Research Office. Most of the tests were performed by H. L. Duhamel.

REFERENCES

1. R. J. Farris and J. E. Fitzgerald, Deficiences of viscoelastic theories as applied to solid propellants. Bull. JANNAF Mech. Beh. Wkg. Group, 8th Mtg., CPIA Pub. 193 (March 1970).
2. R. J. Farris, The stress–strain behavior of mechanically degradable polymers. In *Polymer Networks: Structural and Mechanical Properties* (Edited by A. J. Chompff and S. Newman). Plenum New York (1971).
3. W. F. Briggs, E. C. Francis and D. Gutierrez-Lemini, Some considerations in modeling nonlinear materials with damage. *Proc. 17th Mtg. Soc. Engng Sci.*, Georgia Institute of Technology, (Dec. 1980).
4. W. L. Hufferd, J. E. Fitzgerald and A. U. Sulijoadikusumo, Permanent memory effects in solid propellants. UTEC CE 73-217, *Proc. 1974 Combined JANNAF Structures and Mech. Behavior and Operational Serviceability Working Groups*. CPIA Pub. 253, Johns Hopkins Univ. (July 1974).
5. E. C. Francis and C. H. Carlton, Some aspects of nonlinear mechanical behaviour of a composite propellant. *J. Spacecraft Rockets* **6**, 65–69 (1969).
6. M. E. Gurtin and E. C. Francis, On a simple rate-independent model for damage. *J. Spacecraft Rockets* **18**, 285–286 (1981).
7. H. Cristescu, *Dynamic Plasticity*. North Holland, Amsterdam (1976).
8. M. J. Quinlan, Materials with variable bonding. *Arch. Rat. Mech. Anal.* **68**, 165–181 (1978).
9. S. R. Swanson, L. W. Christensen and R. J. Christensen, A nonlinear constitutive law for propellant. Forthcoming.
10. L. Mullins, Softening of rubber by deformation. *Rubber Chem. Tech.* **42**, 339–362 (1969).
11. R. J. Farris, L. R. Hermann, J. R. Hutchinson and R. A. Schapery, Development of a solid rocket propellant nonlinear viscoelastic constitutive theory. Final Rep. AFRPL-TR-75-20, Aerojet Solid Propulsion Co., (May 1975).
12. R. A. Schapery, On constitutive equations for viscoelastic composite materials with damage. *Workshop on a Continuum Mechanics Approach to Damage and Life Prediction*. Sponsored by NSF, Carrollton, Kentucky (May 1980).
13. M. E. Gurtin, On a simple nonlinear model for viscoelastic materials that exhibit stress softening. AFOSR Rep. Department of Mathematics, Carnegie-Mellon U. (Jan. 1981).
14. R. L. Peeters and R. M. Hackett, Constitutive modelling of plastic-bonded explosives. *Experimental Mech.* **21**, 111–116 (1981).